JOURNAL OF MATERIALS SCIENCE 36 (2001) 4137–4143

Oxidation behavior of Si-C-O fibers (Nicalon) in alumina

T. SHIMOO, K. OKAMURA
Department of Metallurgy and Materials Science, Graduate School of Engineering, Osaka Prefecture University, 1-1, Gakuen-cho, Sakai, Osaka 599-8531, Japan

T. YAMANAKA
Graduate Student, Osaka Prefecture University, 1-1, Gakuen-cho, Sakai, Osaka 599-8531, Japan

Porous Nicalon–alumina compacts with a bulk density of 2.32 Mg/m^3 were oxidized in Ar-25%O_2 gas mixture at 1373–1773 K, and subsequently they were exposed to argon at 1773 K. The mass change of compacts was thermogravimetrically determined during oxidation and exposure. The oxidized and exposed fibers were characterized through AES and XRD analysis. As the oxidation temperature increased, the oxide film was successively transformed into amorphous silica, cristobalite and mullite. The fiber core was only slightly decomposed during oxidation above 1473 K. The oxidation rate could be described by the two-dimensional disc-contracting formula: reaction control at earliest stage and diffusion control at later stage. The oxidation of Nicalon was greatly accelerated by the presence of alumina. Excess thickening in oxide film caused the thermal decomposition of the fiber core during exposure in argon: >0.8 μm for cristobalite film and >1.5 μm for mullite film.

1. Introduction

In order to improve the performance of structural ceramics for high-temperature applications, polycarbosilane-derived Si-C-O fiber (Nicalon, Nippon Carbon Co., Tokyo, Japan) is often employed as a reinforcing material for ceramic-matrix composites. The oxidation of reinforcing fibers may have serious influence on the thermal stability of composites. Therefore, investigations have been made of the oxidation behavior of Nicalon fibers in composites [1–5]. A carbon-rich interfacial layer is formed on oxidation of Nicalon fibers during hot pressing of glass-ceramic composites, providing a strong bond between the fibers and the matrix [1]. When heated in oxidizing environments, the composites lose their strength and exhibit brittle failure because of the oxidation of the carbon-rich interlayer to a silica-rich interlayer. Although the oxidation rates of Nicalon in composites were not measured, they were concluded to be limited by the inward diffusion of oxygen in silica layer [2, 3]. The oxidation of a Nicalon-reinforced magnesium aluminosilicate caused a mass gain, showing the parabolic behavior against time [4]. Recently, the oxidation of BN/Nicalon-reinforced alumina-matrix in air was investigated through microstructure and strength of fibers [5].

A deeper understanding of the performance of Nicalon-reinforced ceramic-matrix composites will be acquired by studying the oxidation kinetics of the fibers in ceramic-matrix and the interaction between the fibers and the matrix in oxidizing environments at high temperatures. The silica film has a suppression effect on the thermal decomposition of the unoxidized fiber core in inert atmosphere at elevated temperatures [6]. Therefore, a knowledge of suppression effect in composites also is very attractive. In this study, Nicalon fibers embedded in alumina powder were oxidized in Ar-25%O_2 gas mixtures at the temperature range from 1373 K to 1773 K and subsequently exposed in argon at 1773 K to examine the formation of oxide film, oxidation kinetics and thermal stability of oxidized fibers. Such information may be of an aid in the clarification of the oxidation behavior of Nicalon-reinforced ceramic-matrix composites.

2. Experimental method

The samples used in this study are Si-C-O fiber (Nicalon 202, Nippon Carbon Co., Japan) and alumina powder (Taimicron TM-DAR, Taimei Chemicals Co., Japan). Nicalon fiber has a mean diameter of 15 μm and a composition of $SiC_{1.20}O_{0.41}$. Alumina powder has an α-type crystal structure, a mean particle size of 0.21 μm and a purity of 99.99%, and contains the following impurities: 12 ppm Si, 5 ppm Fe, 3 ppm Na, 1 ppm K, 1 ppm Ca and 1 ppm Mg. In addition, this powder has excellent sinterability. One gram Nicalon fibers and 1 g alumina powder were thoroughly mixed by grinding in an alumina mortar. The Nicalon-alumina mixture was formed into a tablet of 15 mm in diameter by compacting under a pressure of 9.8 MPa at room temperature. The porous compact with a bulk

density of 2.32 Mg/m^3 contained chop-like fibers of 100–200 μm in length.

A platinum crucible, in which the compact was placed, was connected to an auto-recording balance with a platinum wire and was suspended in the hot zone of an SiC resistance furnace regulated at a given temperature. Ar-25%O_2 gas mixture was introduced in an alumina reaction tube at flow rate of 2.5×10^{-5} m^3/s. The compact was oxidized at temperature ranging from 1373 to 1773 K and for time ranging from 0.9 to 36 ks. To investigate the thermal stability of Nicalon fibers in the compact, the oxidized compact was submitted to the exposure test at high temperature. Using an SiC resistance furnace, the oxidized Nicalon-alumina compact was heated in a platinum crucible for 36 ks at 1773 K in flowing argon gas of 2.5×10^{-5} m^3/s.

The mass change of the compact was continuously monitored during oxidation and exposure. The existing phases in both the oxidized and exposed compacts were examined by X-ray diffractometry, using Cu K_α radiation. The surface composition of the oxidized fibers was determined by Auger spectrometric analyzer.

3. Result and discussion

3.1. Oxidation of Nicalon fibers in alumina

Fig. 1 shows TG curves for Nicalon fibers-alumina powder compacts oxidized in Ar-25%O_2 gas mixture at 1373–1773 K. ΔW and W_0 are the mass gain measured by TG and the initial mass of fibers in compact, respectively. Observed mass gains are due to the oxidation of Nicalon fibers which is expressed by the overall reaction:

$$SiC_{1.20}O_{0.41}(s) + 1.395O_2(g) = SiO_2(s) + 1.20CO(g) \quad (1)$$

TG curves for the oxidation of Nicalon fibers alone under identical conditions also are shown in Fig. 1 [7]. The oxidation rates of Nicalon in alumina were large compared to that of Nicalon alone. Particularly, it may be noted that the oxidation of Nicalon was greatly accelerated by the rise in temperature from 1673 to 1773 K.

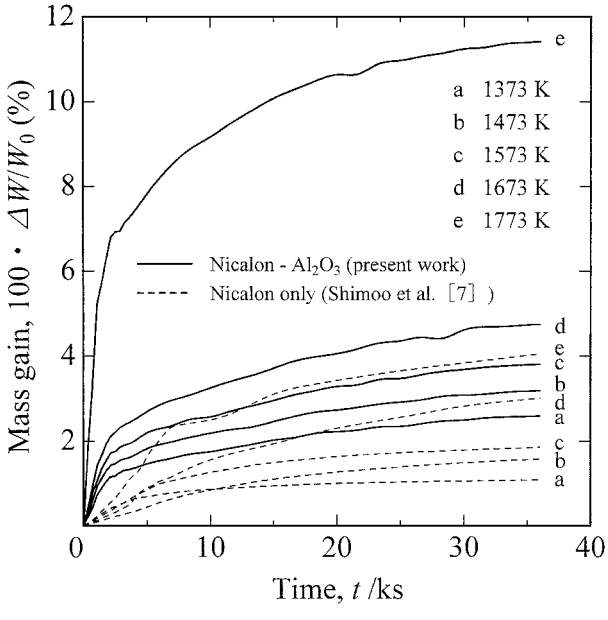

Figure 1 TG curves for oxidation of Nicalon-alumina compacts.

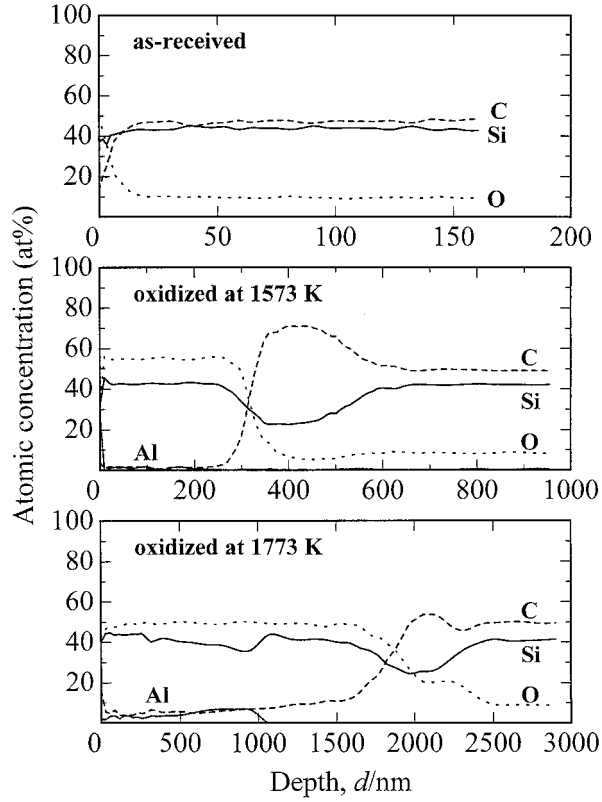

Figure 2 AES depth profiles of as-received fibers and fibers in compacts oxidized at 1573 and 1773 K.

Fig. 2. shows the AES depth profiles of as-received fiber and fibers in the compacts oxidized at 1573 and 1773 K. The fibers oxidized at 1573 K were coated with an SiO_2 film of about 300 nm thickness. The SiO_2 film contained a slight amount of aluminum. After oxidation at 1773 K, the SiO_2 film became thicker up to about 1700 nm and contained 5–10 at% Al. There was a carbon-enriched layer of about 200 nm thickness between the oxide film and the unoxidized core. For the oxidation of Nicalon alone, such the layer was observed only under low oxygen partial pressure ($p_{O2} = 2 \times 10$ Pa) [8]. Possibly the oxygen partial pressure was lowered at the oxide-core interface, being favorable for the occurrence of the following reaction:

$$SiC_{1.20}O_{0.41}(s) + 0.795O_2(g) = SiO_2(s) + 1.20C(s) \quad (2)$$

X-ray diffraction patterns of the oxidized Nicalon-alumina compacts are shown in Fig. 3. The SiO_2 film formed around fibers was amorphous below 1473 K, and it crystallized into cristobalite above 1573 K (see the sharp peak at $2\theta \fallingdotseq 23°$). For the fibers oxidized at 1773 K, mullite was produced in addition to cristobalite. Using Scherrer's formula, the apparent crystallite size of β-SiC, D_{SiC}, was calculated from the half-value width of the diffraction peak at $2\theta \fallingdotseq 60°$. Fig. 4. shows the relationship between D_{SiC} and oxidation temperature. Nicalon fibers have a microstructure consisting of β-SiC crystallites, free carbon and amorphous silicon oxycarbide (SiC_XO_Y) phase. The SiC_XO_Y phase,

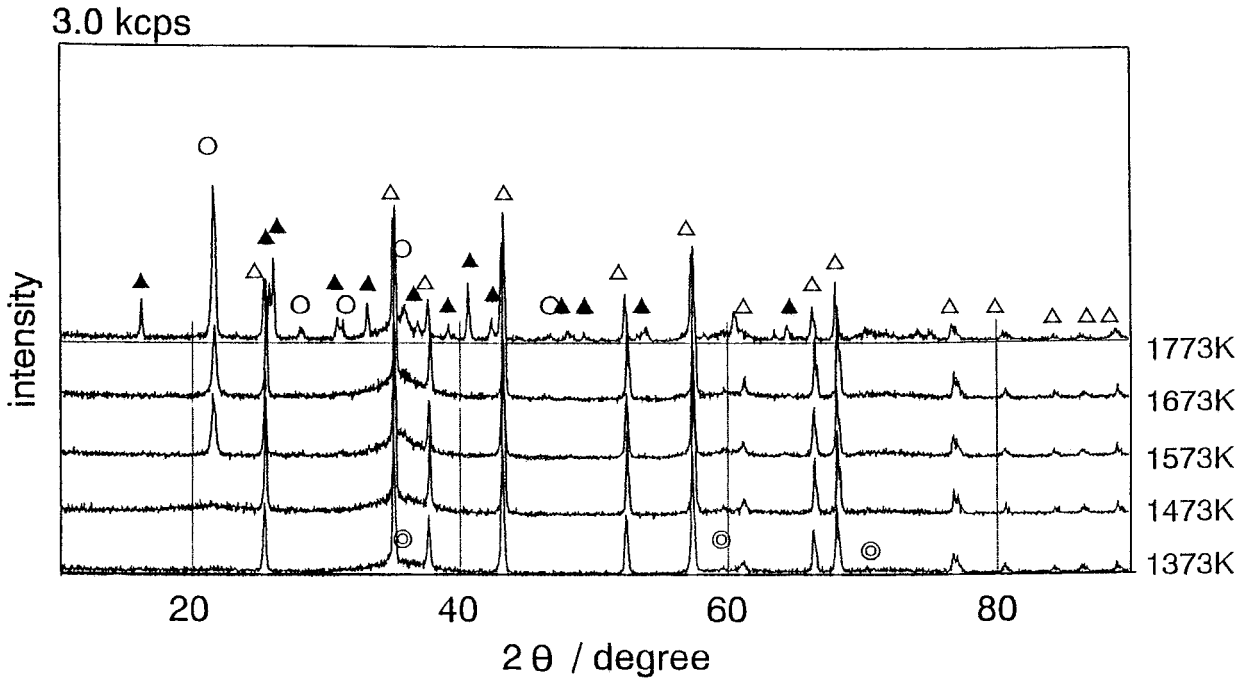

Figure 3 X-ray diffraction patterns of Nicalon-alumina compacts oxidized for 36 ks at different temperature. ○ cristobalite, ⊙ SiC, △ alumina, ▲ mullite.

which is unstable at elevated temperature, has a tendency to crystallize into β-SiC and generate SiO and CO gases, resulting in the growth of β-SiC crystallites. Therefore, in inert gas and above 1473 K, Nicalon fibers are thermally decomposed by the overall reaction:

$$SiC_{1.20}O_{0.41}(s) = 0.895SiC(s) + 0.105SiO(g) + 0.305CO(g) \quad (3)$$

The thermal decomposition of Nicalon fibers, as well as in inert gas, should occur in the oxidizing environment. This was verified by the gradual increase in the value D_{sic} above 1473 K, implying that the thermal decomposition of Nicalon occurred slightly during the oxidation of compacts.

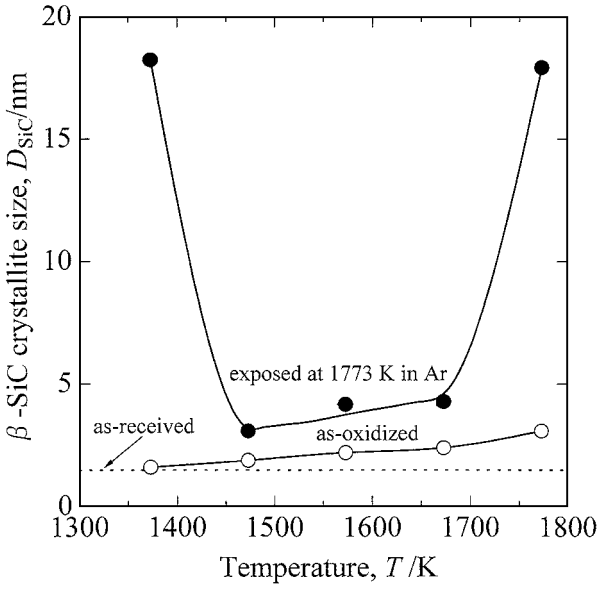

Figure 4 Relationship between β-SiC crystallite size of Nicalon in compacts oxidized for 36 ks and oxidation temperature.

Mullite is thought to be produced by the reaction of cristobalite formed around fibers with alumina powder:

$$3Al_2O_3(s) + 2SiO_2(s) = 3Al_2O_3 \cdot 2SiO_2(s)$$
$$\Delta G^\circ/\text{cal} \cdot \text{mol}^{-1} = 2055–4.16T/\text{K}\,[9] \quad (4)$$

Thermodynamics consideration indicates that reaction (4) can proceed above 494 K. In addition, the Al_2O_3-SiO_2 phase diagram shows that the SiO_2 and mullite phases coexist at equilibrium below 1868 K [10]. Therefore, aluminum as mullite is present in the oxide film. Obviously, X-ray diffraction indicates that the oxide film at 1773 K consists of the SiO_2 and mullite phases. On the other hand, no mullite could be detected at 1573 K, though aluminum was contained in the oxide film. This seems to be because the mullite content in the oxide film is outside the limits of identification by X-ray diffraction.

To reveal the formation of mullite at 1773 K, Nicalon fibers were oxidized in alumina in a given time ranging from 0.9 to 10.8 ks. Fig. 5 shows the X-ray diffraction patterns of the oxidized samples. While the X-ray diffraction peaks of cristobalite were already found by the oxidation of 0.9 ks, those of mullite appeared after oxidation of 2.7 ks. The peaks of cristobalite and mullite became sharper by prolonging oxidation time.

Fig. 6 shows the relationship between the value D_{SiC} and oxidation time. Although β-SiC crystallite size increased slightly within about 5 ks, it remained almost unchanged by prolonging the oxidation time. This result indicates that thickening in the oxide film is necessary for suppressing the thermal decomposition of fibers during oxidation.

3.2. Oxidation kinetics of Nicalon in alumina

The initial oxidation rate of SiC fibers was controlled by the reaction at the fiber surface, being described

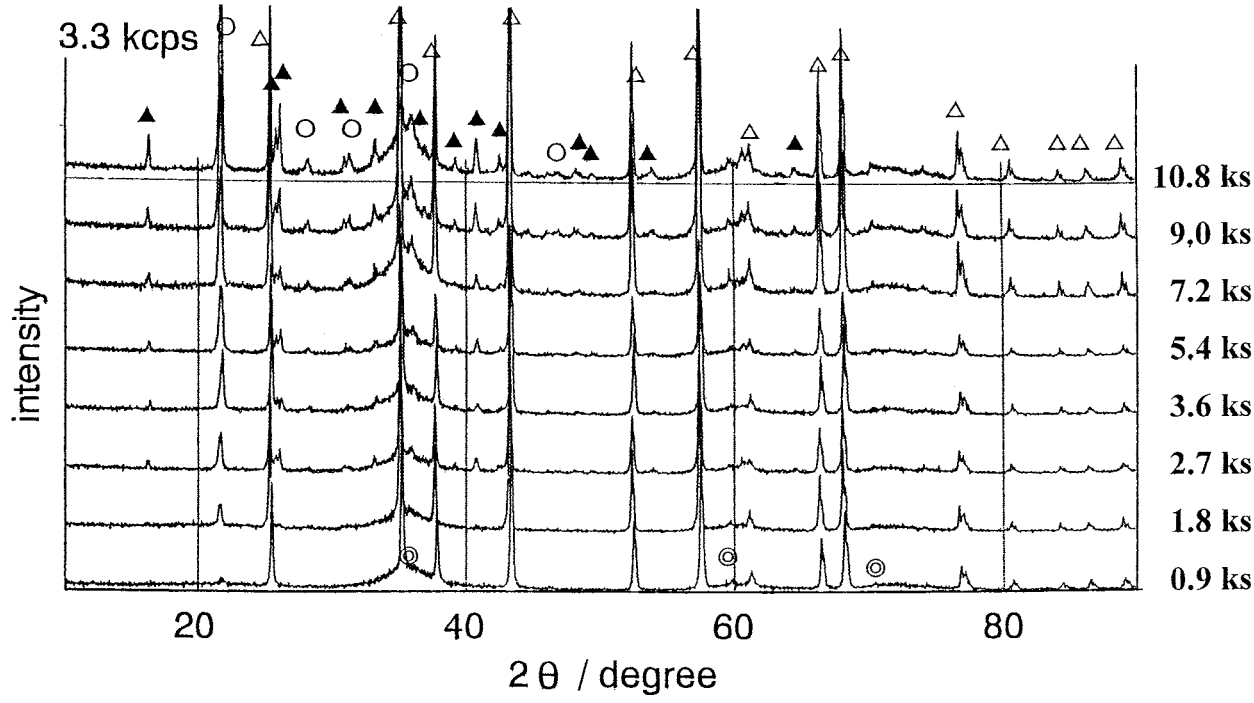

Figure 5 X-ray diffraction patterns of Nicalon-alumina compacts oxidized for different times at 1773 K. ○ cristobalite, ◎ SiC, Δ alumina, ▲ mullite.

by the following two-dimensional disc-contracting rate equation [7, 11]:

$$1 - (1 - X)^{1/2} = k_r t \tag{5}$$

When the fibers were completely coated with oxide film, the oxidation rate was described by the two-dimensional contracting disc formula for diffusion control [7, 11]:

$$(1 - X)\ln(1 - X) + X = k_d t \tag{6}$$

where k_r and k_d are the rate constants. From the stoichiometry of reaction (1), the oxidized fraction of fibers, X is given by Equation 7:

$$X = 4.435 \cdot \Delta W / W_0 \tag{7}$$

Figs 7 and 8 show the application of rate equation (5) and (6) to TG data shown in Fig. 1. The linear relationship between $1 - (1 - X)^{1/2}$ and time, t, held within about 1 ks (that is, in the earliest stage of oxidation). After about 5 ks of oxidation, the plots of $(1 - X)\ln(1 - X) + X$ versus t gave a linear relationship at 1173–1673 K. For this temperature range, the oxide film was amorphous silica and cristobalite. At 1773 K, no linear relationship found to hold between $(1 - X)\ln(1 - X) + X$ and t. This seems to be because the permeability of the oxide film to oxygen may be

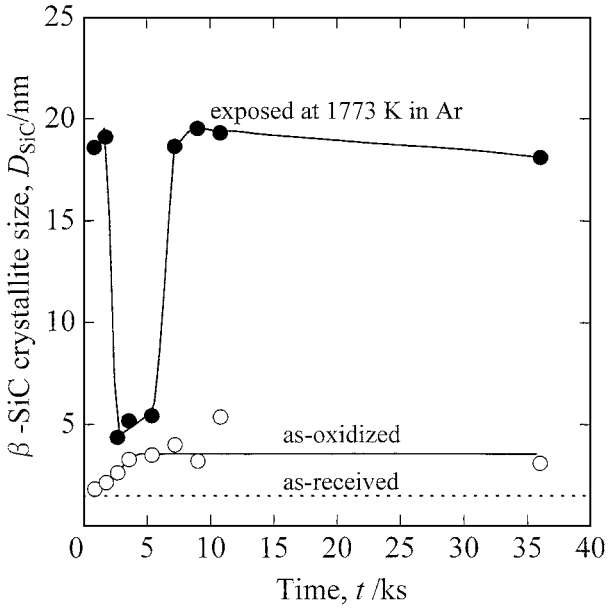

Figure 6 Relationship between β-SiC crystallite size of Nicalon in compacts oxidized at 1773 K and oxidation time.

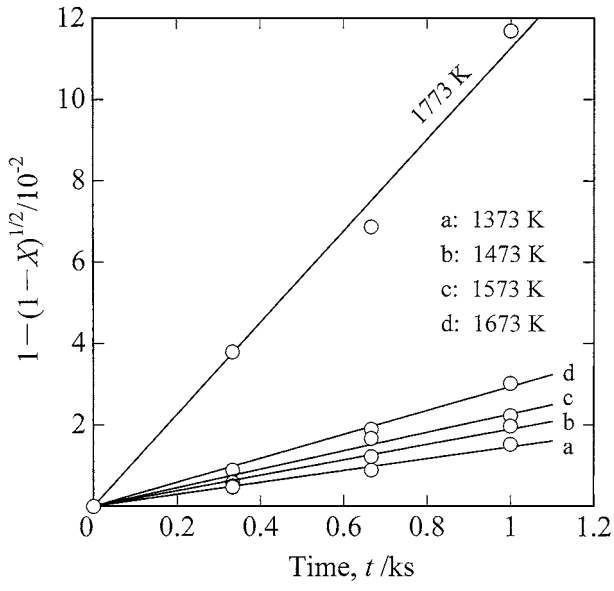

Figure 7 Application of two-dimensional contracting-disc formula for reaction control to rate data shown in Fig. 1.

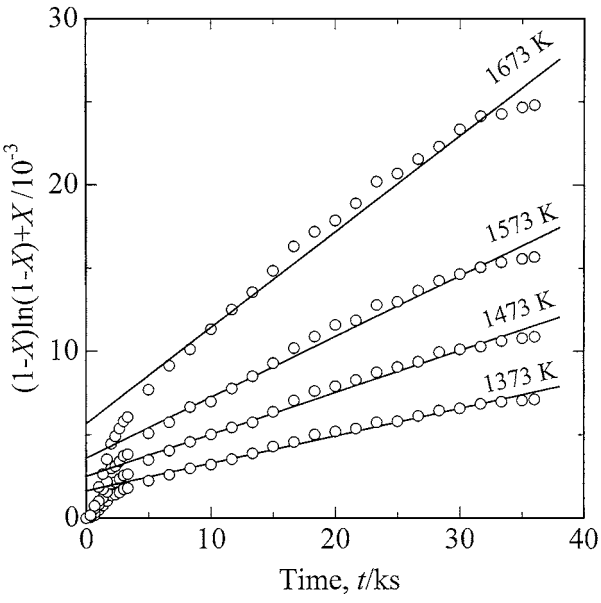

Figure 8 Application of two-dimensional contracting-disc formula for diffusion control to rate data shown in Fig. 1.

altered significantly by the transition from cristobalite to mullite with the period of the oxidation time.

The temperature dependences of the rate constants, k_r and k_d, are shown in Fig. 9 by the Arrhenius plots. The activation energies were estimated to be 43 kJ/mol for reaction control and 96 kJ/mol for diffusion control, respectively. The Arrhenius plots of k_r and k_d also are shown in Fig. 9 for the oxidation of Nicalon fibers alone [7]. The activation energies of 45 kJ/mol for reaction control and 102 kJ/mol for diffusion control are comparable to those for the oxidation of Nicalon in alumina. Therefore, the oxidation rate of Nicalon in alumina, as well as that of Nicalon alone, is determined by the same oxidation mechanism. In particular, the diffusion species through the oxide film are oxygen molecules [7].

The values of k_r and k_d are larger for the Nicalon in alumina than for Nicalon alone; about 2 times for k_r in the temperature range of 1373–1673 K, about 5 times for k_r at 1773 K and 3–4 times for k_d. As described below, this seems to be because alumina itself, and potassium and sodium in it accelerate the oxidation of Nicalon fibers as well as that of SiC ceramics [12–15].

The oxidation behavior of SiC ceramics is determined predominantly by the nature and concentration of the hot-pressing additives (alumina) and the impurity elements rather than by the intrinsic oxidation of SiC to SiO_2 [12]. Alumina diffuses into the SiO_2 film to form alumino-silicates. The alumino-silicates have higher oxygen permeability than pure silica, presumably leading to higher oxidation rate [13]. In addition, low levels of sodium and potassium (~ppm) can open up the silica network and allow faster transport of oxygen molecules. Oxidation rates of SiC ceramics are increased by up to an order of magnitude in such environments [14]. AES depth profiles for Nicalon fibers oxidized in alumina powder indicate the formation of mullite. In addition, alumina powder employed in this study contains 3 ppm sodium and 1 ppm potassium. Therefore, both the effects on improvement for permeability of oxygen molecules to silica film led to the increase in the rate constant for diffusion control, k_d. The impurities and additives leads to different microstructures of silica films, resulting in different rate constants for reaction control, k_r, in the oxidation of SiC ceramics [15]. There is the possibility that the value k_r for the oxidation of Nicalon fibers increased by the presence of alumina, sodium and potassium.

3.3. Exposure of oxidized fibers in argon

When Nicalon fibers were exposed in inert gas at elevated temperature, the oxide film had the suppression effect for the thermal decomposition of fiber core [6]. Whether the oxide film formed in alumina powder has the same effect or not was investigated. The oxidized

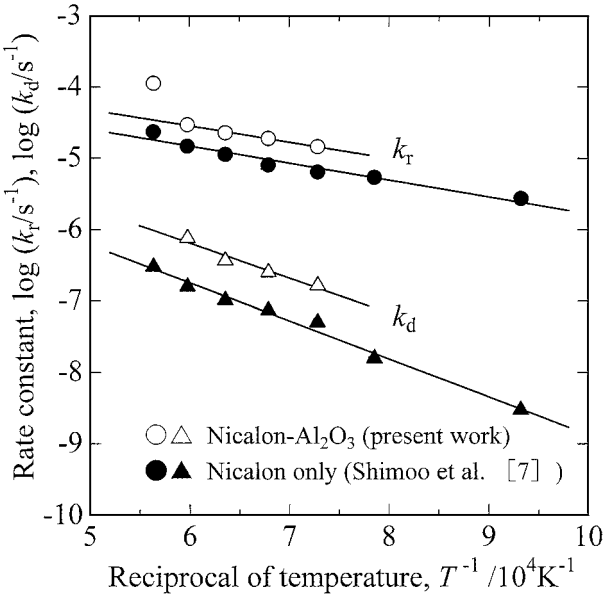

Figure 9 Arrhenius plots for rate constants, k_r and k_d.

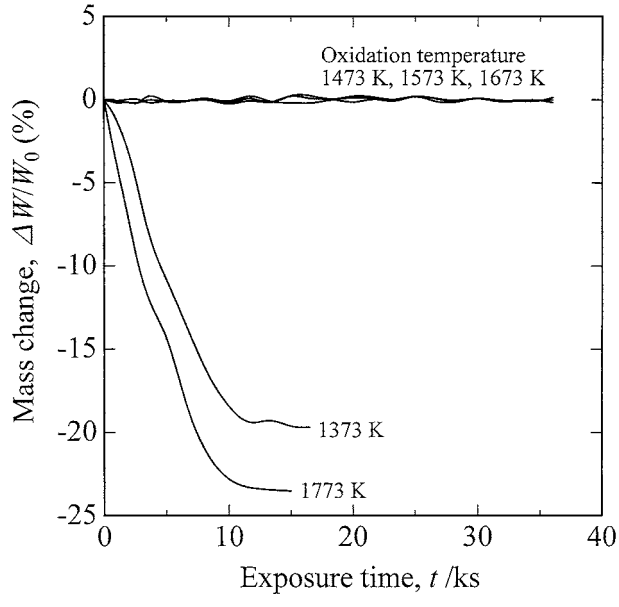

Figure 10 TG curves of Nicalon-alumina compacts exposed at 1773 K in Ar (previously oxidized for 36 ks at different temperatures).

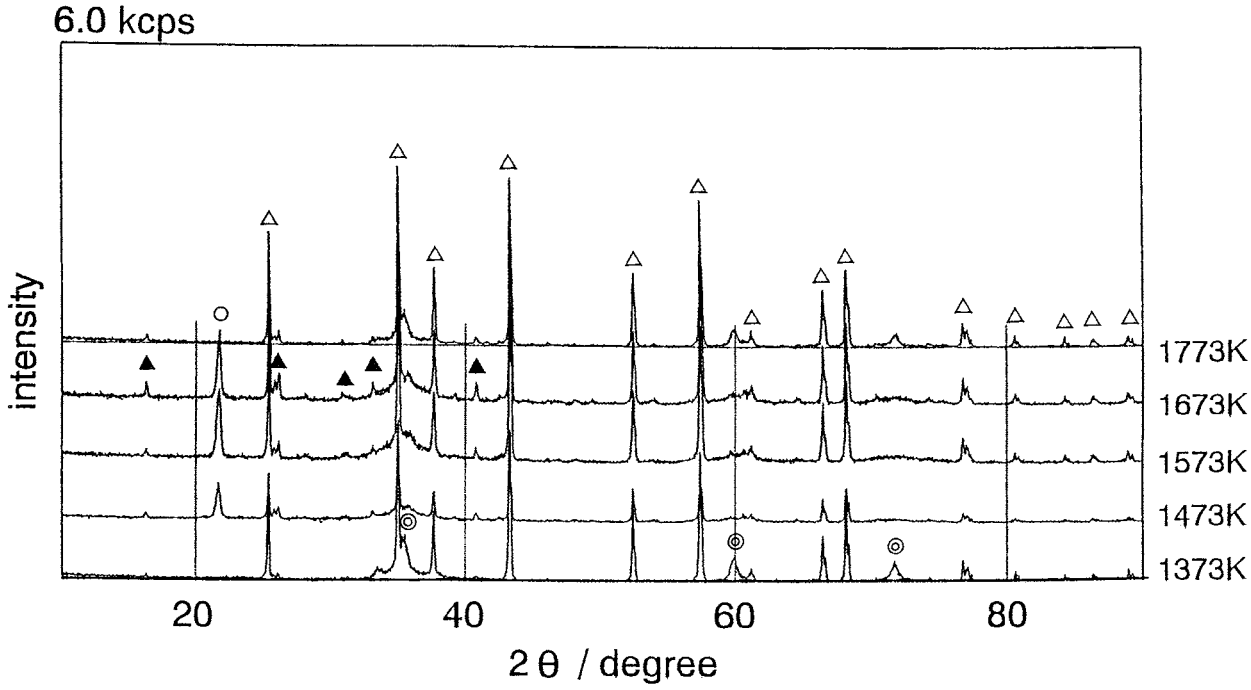

Figure 11 X-ray diffraction patterns of Nicalon-alumina compacts oxidized for 36 ks at different temperatures and subsequently exposed at 1773 K in Ar. ○ cristobalite, ◎ SiC, △ alumina, ▲ mullite.

Nicalon-alumina compacts were exposed at 1773 K in argon.

Fig. 10 shows the TG curves during exposure for the Nicalon–alumina compacts oxidized at 1373–1773 K. No mass change was observed for the fibers oxidized at 1473, 1573 and 1673 K. On the other hand, there was a significant decrease of 20–24% in the mass of the compacts oxidized at 1373 and 1773 K. The XRD patterns of the exposed compacts are shown in Fig. 11. β-SiC peaks in the compact samples oxidized at 1373 and 1773 K were much sharper after exposure than in the as-oxidized state (Fig. 3). As can be seen from Fig. 4, the thermal decomposition of fiber core (reaction (3)) caused the coarsening of the β-SiC grains. In addition, while the peaks of silica and mullite became obscure, the alumina peak became sharp. These results imply the disappearance of the oxide film (silica and mullite), according to the following reactions:

$$SiO_2(s) + CO(g) = SiO(g) + CO_2(g) \quad (8)$$

$$3Al_2O_3 \cdot 2SiO_2(s) + 2CO(g) = 3Al_2O_3(s) + 2SiO(g) + 2CO_2(g) \quad (9)$$

For the samples oxidized at 1473, 1573 and 1673 K, the cristobalite peaks were retained and β-SiC peaks remained broad. By considering no mass loss (Fig. 10), it is evident that the oxide film suppressed the decomposition of the core during exposure in argon. Consequently, β-SiC crystallite grew only slightly after exposure at 1773 K in argon. By comparing Fig. 3 and Fig. 11, it can be seen that mullite was produced by the interaction of silica film with alumina powder even during exposure in argon at 1773 K.

Figs 12 and 13 show the TG curves and XRD patterns for the compacts exposed at 1773 K in argon against the oxidation time, respectively. No mass change, broad β-SiC peaks and sharp cristobalite peaks for the compacts oxidized for 2.7–5.4 ks indicate that no decomposition of Nicalon fibers was caused by the exposure in argon. Therefore, as can be seen from Fig. 6, β-SiC crystallite grew only slightly after exposure. The significant mass loss (Fig. 12), the disappearance of cristobalite peaks, weakening in mullite peaks (Figs 5 and 13) and the coarsening of β-SiC crystal (Fig. 6) were observed after exposure of <1.8 ks and >7.2 ks. This is because the occurrence of reactions (3), (8) and (9) led to the decomposition of Nicalon fibers and the reduction of oxide film by CO gas. Adequate thickness of oxide film was efficient in suppressing the decomposition of SiC_XO_Y phase by restricting the outward

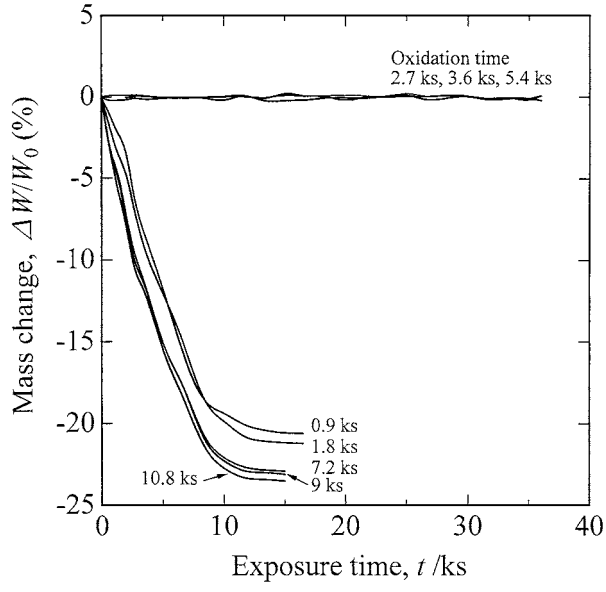

Figure 12 TG curves of Nicalon-alumina compacts exposed at 1773 K in Ar (previously oxidized for different times at 1773 K).

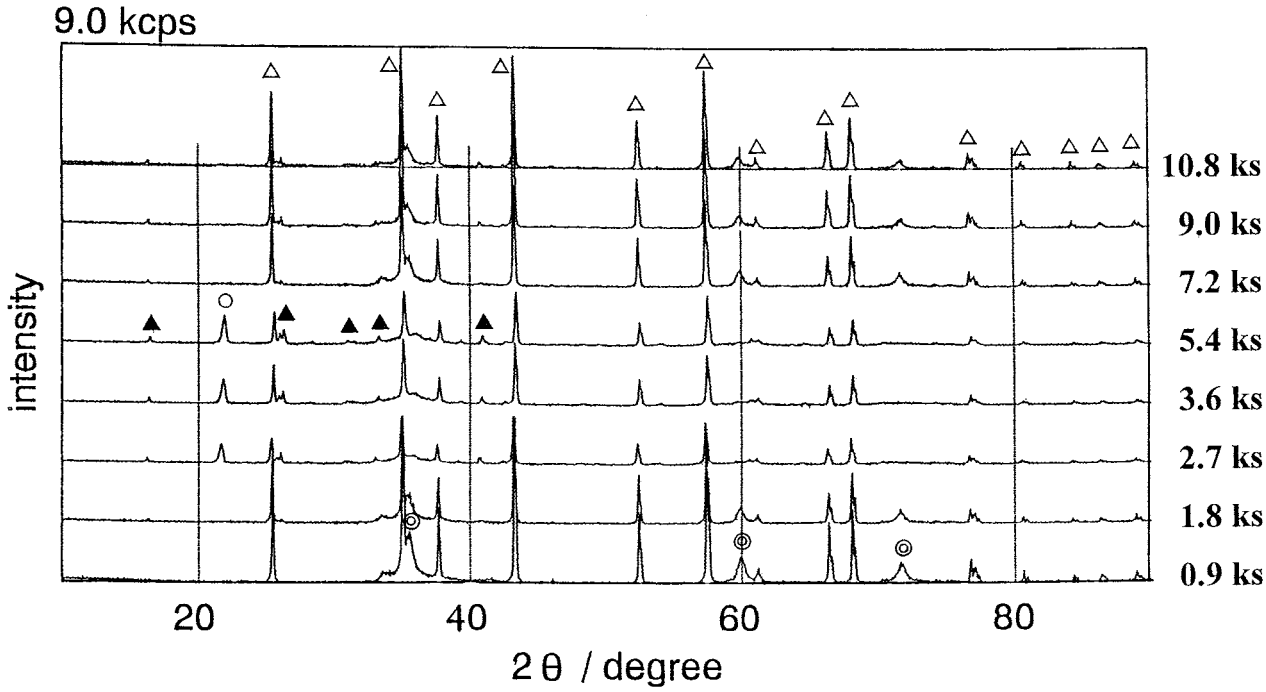

Figure 13 X-ray diffraction patterns of Nicalon-alumina compacts oxidized for different times at 1773 K and subsequently exposed at 1773 K in Ar. ○ cristobalite, ◎ SiC, △ alumina, ▲ mullite.

transport of the decomposition gases, SiO and CO. However, when the oxide layer became too thick as a result of long time oxidation at higher temperatures, the decomposition of fiber core was caused by the formation of imperfections such as cracks and bubbles [6, 16]. The thickness of oxide film, b, is approximately estimated by the following equation:

$$b = r_0 \cdot \{1 - (1 - X)^{1/2}\} \qquad (10)$$

where r_0 is the initial radius of Nicalon fiber (=7.5 μm). The maximum thickness of the oxide film, by which the thermal decomposition of fiber core could be suppressed, was 0.8 μm for cristobalite and 1.5 μm for cristobalite + mullite, respectively. It was found that mullite has excellent suppression effect on the decomposition of Nicalon fibers compared to cristobalite.

4. Conclusion

Silica film reacted with aluminum, resulting in the formation of mullite. The oxidation rate of Nicalon in alumina obeyed the two-dimensional disc-contracting rate equation for reaction control at earliest stage of oxidation, and subsequently it obeyed that for diffusion control. The activation energies were 43 kJ/mol and 96 kJ/mol, respectively. Although the oxidation of Nicalon fibers were greatly accelerated by the presence of alumina, the oxidation mechanism was identical to that of Nicalon alone. When exposed in argon, the thermal decomposition of fiber core was suppressed by controlling the oxide film thickness. Excess oxidation caused the decomposition of fiber core and the disappearance of oxide film during exposure in argon.

Acknowledgements

This study was supported in part by the Ministry of Education, Science, Sports and Culture under Grant No. 11450255.

References

1. R. F. COOPER and K. CHYUNG, *J. Mater. Sci.* **22** (1987) 3148.
2. E. BISHOFF, M. RÜHLE, O. SBAIZERO and A. G. EVANS, *J. Amer. Ceram.* **72** (1989) 741.
3. L. A. BONNEY and R. F. COOPER, *ibid.* **73** (1990) 2916.
4. A. KUMAR and K. M. KNOWLES, *ibid.* **79** (1996) 2364.
5. J. P. RIGUEIRO, J. A. CELEMÍN and J. LLORCA, *ibid.* **82** (1999) 3494.
6. T. SHIMOO, F. TOYODA and K. OKAMURA, *J. Ceram. Soc. Jpn.* **107** (1999) 263.
7. *Idem., ibid.* **106** (1998) 447.
8. T. SHIMOO, Y. MORISADA and K. OKAMURA, *J. Amer. Ceram. Soc.* **83** (2000) 3049.
9. E. T. TURKDOGAN, "Physical Chemistry of High Temperature Technology" (Academic Press, New York, 1980) p. 5.
10. R. S. ROTH, T. NEGAS and L. P. COOK (Eds.), "Phase Diagrams for Ceramists," Vol. IV (The American Ceramic Society, Columbus, 1981) p. 116.
11. T. SHIMOO, F. TOYODA and K. OKAMURA, *J. Mater Sci.* **35** (2000) 3301.
12. S. C. SINGHAL, *ibid.* **11** (1976) 1246.
13. M. A. LaLAMKIN, F. L. RILEY and R. L. FORDHAM, *J. Eur. Ceram. Soc.* **10** (1992) 347.
14. V. PAREEK and D. A. SHORES, *J. Amer. Ceram. Soc.* **74** (1991) 556.
15. T. NARUSHIMA, T. GOTO, Y. IGUCHI and T. HIRAI, *ibid.* **73** (1990) 3580.
16. H.-E. KIM and A. J. MOORHEAD, *ibid.* **74** (1991) 666.

Received 3 August 2000
and accepted 7 May 2001